Interspecific Bergmann's rule pattern in birds persists despite seasonal migration

[1*]Ayumi Mizuno, [1]Erick J. Lundgren, [2,3]Szymon M. Drobniak, [4]Corey T. Callaghan, [1]Eduardo S.A. Santos, [1,2]Malgorzata Lagisz, [1]Santiago Ortega, [1]Xi Lin, and [1,2] Shinichi Nakagawa

[1] Collaboration for Open Science and Synthesis in Ecology and Evolution (COSSEE), Department of Biological Sciences, Faculty of Science, University of Alberta, Edmonton, Canada
[2] Evolution and Ecology Research Centre, School of Biological, Earth and Environmental Sciences, University of New South Wales, Sydney, New South Wales, Australia
[3] Institute of Environmental Sciences, Faculty of Biology, Jagiellonian University, Kraków, Poland
[4] Department of Wildlife Ecology and Conservation, Fort Lauderdale Research and Education Center, University of Florida

Corresponding author
Ayumi Mizuno, ayumi.mizuno5@gmail.com

ORCID ID
Ayumi Mizuno: 0000-0003-0822-5637
Erick J. Lundgren: 0000-0001-9893-3324
Szymon M. Drobniak: 0000-0001-8101-6247
Corey T. Callaghan: 0000-0003-0415-2709
Eduardo S.A. Santos: 0000-0002-0434-3655
Malgorzata Lagisz: 0000-0002-3993-6127
Santiago Ortega: 0000-0002-3518-276X
Xi Lin: 0000-0001-9271-9415
Shinichi Nakagawa: 0000-0002-7765-5182

Author contributions
Conceptualization: AM, SN
Methodology: AM, SN, EL, SMD
Formal analysis: AM
Investigation: AM
Data curation: AM, EL
Writing - original draft: AM
Writing - Review & Editing: All
Visualization: AM
Supervision: AM, SN
Project administration: AM, SN
Funding acquisition: AM, SN

Data availability
Data and analysis scripts can be found at https://github.com/Ayumi-495/bergmann-migratory and https://doi.org/10.5281/zenodo.21687159.

Funding
AM: JSPS Overseas Research Fellowship (202660034)
ML: NSERC Discovery Grant (RES0074477)
CTC: USDA Hatch (FLA-FTL-006297)
SN: Canada Excellence Research Chair (CERC-2022-00074) and NSERC Discovery Grant (RGPIN-2025-04813)

Acknowledgements
We acknowledge BirdLife International and Handbook of the Birds of the World for providing the *Bird species distribution maps of the world*, Version 2025.2, used in this study. A.M. was supported by a Japan Society for the Promotion of Science Overseas Research Fellowship (202660034). M.L. was supported by a Natural Sciences and Engineering Research Council of Canada Discovery Grant (RES0074477). C.T.C. was supported by the USDA National Institute of Food and Agriculture Hatch project FLA-FTL-006297. S.N. was supported by a Canada Excellence Research Chair award (CERC-2022-00074) and a Natural Sciences and Engineering Research Council of Canada Discovery Grant (RGPIN-2025-04813).

Conflict of interest
None

Declare of AI use
During the preparation of this manuscript, the authors used ChatGPT 5.5 (OpenAI) and Claude Opus 4.8 (Anthropic) to assist with the development and revision of R scripts and with English-language editing and proofreading. All AI-generated suggestions, text, and code were critically reviewed, verified, and revised by the authors before use. The authors made all decisions regarding the study design, data analysis, interpretation of the results, and presentation of the conclusions. The authors take full responsibility for the accuracy, integrity, and originality of the manuscript and its associated analyses and code.

Abstract (200 words)

Climatic gradients are thought to shape animal body size, with larger species often occurring in colder environments. Yet trait-climate relationships may reflect current climatic exposure as well as the evolutionary and biogeographic histories that shaped species' traits. Bergmann's rule illustrates this challenge, and birds provide a useful test because seasonal migration decouples body size from climatic exposure across breeding and non-breeding seasons. We asked whether migration weakens the interspecific Bergmann's rule pattern by reducing the negative temperature-body mass slope, or whether migrants instead differ mainly in average body mass. We analysed body mass and seasonal range-climate data for over 10,000 bird species with phylogenetic linear models, comparing resident and migratory species under breeding- and non-breeding-season climate assignments. Body mass declined with temperature in both residents and migrants under both assignments. Migrants showed a slightly shallower slope, but support for a migrant-resident slope difference was limited. Instead, migrants were consistently smaller than residents after accounting for seasonal climatic exposure, and body mass was lower in migrants with larger seasonal temperature shifts. Thus, migration does not appear to erase Bergmann's rule in birds - migratory species retain a negative temperature-body mass relationship while showing a distinct shift toward smaller body size.

(199/200)

Keywords (3-6)

Ecogeographical rule, biogeography, macroecology, evolutionary inertia

Introduction

Understanding how climate shapes species' traits is central to explaining global biodiversity patterns and predicting biological responses to warming (Millien et al., 2006; Radchuk et al., 2019; Urban et al., 2024). Trait-climate relationships are often used to infer adaptation to environmental gradients, but such inference depends on how climatic exposure is assigned to species. This issue is especially important for species that experience different climates across the annual cycle, because climate summarized from breeding ranges, non-breeding ranges, or year-round ranges may carry different ecological or evolutionary meanings. Ecogeographical rules, including Allen's rule (Allen, 1877), Bergmann's rule (Bergmann, 1847), and Gloger's rule (Delhey, 2019), provide well-known examples of morphology-climate relationships and have been revisited in the context of global climate change (Millien et al., 2006). The key question is not only whether morphology is associated with climate, but which climatic exposure is biologically relevant.

Bergmann's rule highlights this challenge. At the interspecific level, it describes a tendency for larger-bodied species to occur in colder or higher-latitude environments, yet its scope and mechanistic interpretation have long been debated (Bergmann, 1847; Blackburn et al., 1999; Salewski & Watt, 2017). The difficulty is that a temperature-body mass relationship among species does not necessarily imply independent adaptation to current thermal conditions, as closely related species may resemble one another in body size, climatic distributions, or both (Blomberg et al., 2003; Crisp & Cook, 2012; Peterson et al., 1999; Wiens & Graham, 2005).

Birds have been a major focus of empirical tests of Bergmann's rule, with studies investigating Bergmann's rule-like temperature-body mass relationships across different taxonomic, geographic, and analytical scales (Fröhlich et al., 2023; Meiri & Dayan, 2003; Olson et al., 2009). Yet seasonal movement complicates the interpretation of temperature-body mass associations in birds. Comparative studies often assign climate using annual range-wide summaries or breeding-range summaries (Fröhlich et al., 2023; Mainwaring & Street, 2021; Oskyrko et al., 2026), but these choices can assume different evolutionary or ecological pressures when species experience different climates across the annual cycle.

Recent global analyses of avian thermoregulatory morphology illustrate this problem: migratory species have sometimes been excluded from analyses because breeding-range climate alone does not capture temperatures experienced throughout the year (Baldwin et al., 2023). This matters as almost one in five bird species migrate (Somveille et al., 2013). Resident species generally occupy similar geographic ranges year-round, whereas migratory species move between breeding and non-breeding ranges and can experience different climatic conditions across seasons. Particularly in

non-tropical regions, seasonal migration can allow species to avoid harsh conditions in their breeding ranges (Eyres et al., 2020; Somveille et al., 2019). This contrast provides a test of whether temperature-body mass associations primarily reflect current seasonal climatic exposure or broader evolutionary processes.

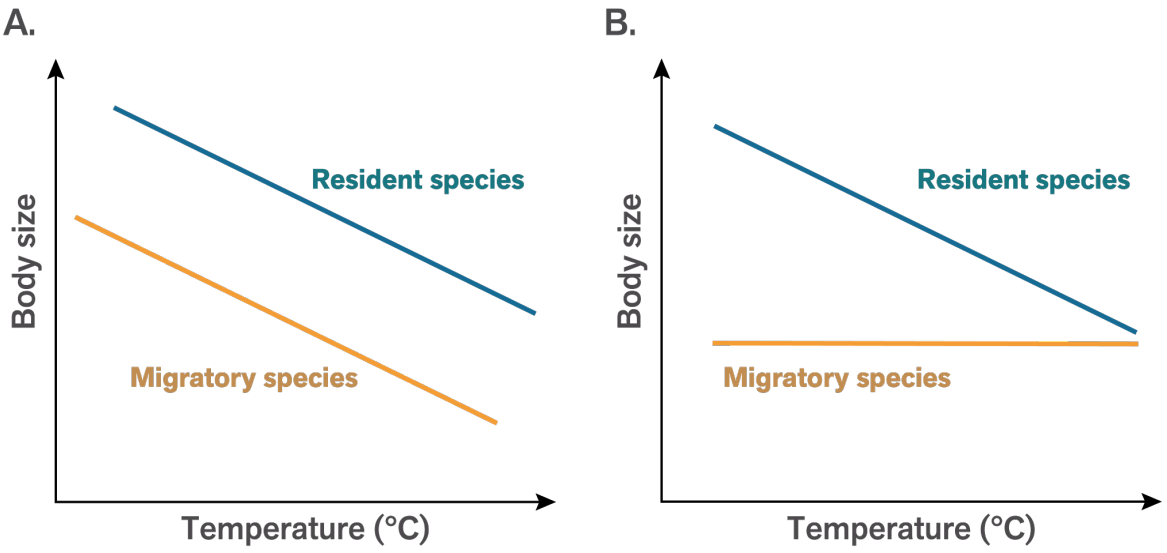

Figure 1. Hypothetical scenarios for using seasonal migration to interpret the interspecific temperature-body mass relationship. (A) If the temperature-body mass relationship is retained despite seasonal movement, migratory species are expected to show a negative relationship similar to that of resident species. Based on previous findings that migratory birds tend to be smaller than non-migratory birds, migratory species may also show a downward shift in average body mass relative to resident species at a given temperature (an average body-mass difference rather than part of the slope-based Bergmann's rule pattern). (B) If the temperature-body mass relationship is weakened by seasonal movement, migratory species are expected to show a shallower negative relationship than resident species because migration can reduce exposure to cold conditions during part of the year.

The resident-migrant contrast provides a way to test whether seasonal movement weakens the temperature-body mass relationship or whether the relationship is retained despite seasonal shifts in climatic exposure (Figure 1). Previous studies have examined whether migratory status is associated with conformity to Bergmann's rule, but have produced mixed results (He et al., 2023; Mainwaring & Street, 2021; Meiri & Dayan, 2003). However, to our knowledge, no previous study has explicitly tested whether the inferred temperature-body mass relationship depends on whether climatic exposure for migratory species is derived from breeding or non-breeding distributions. In our framework, weaker conformity to Bergmann's rule refers specifically to a shallower negative temperature-body mass slope in migratory species. At the same time, migratory birds may retain a similar slope to residents while differing in average body mass. Such an offset

in average body mass would not itself represent weaker conformity to Bergmann's rule, but would indicate a migration-associated difference in body size independent of the temperature-body mass slope. This possibility is consistent with findings that migratory birds tend to be smaller than non-migratory birds, a pattern often interpreted in relation to energetic, aerodynamic, and life-history constraints associated with sustained flight and seasonal movement (Alerstam et al., 2003; Hedenström, 2008; Soriano-Redondo et al., 2020). Separating these two possibilities allows us to ask whether migration weakens the temperature-body mass slope itself and whether it is also associated with an offset in average body mass independent of that slope.

Temperature is the primary climatic axis in Bergmann's rule, but it may not act in isolation. Precipitation can also contribute to body-size variation by reflecting broader ecological conditions such as water availability, productivity, habitat structure, and resource conditions (Ongman et al., 2026; Yom-Tov & Geffen, 2011). Considering precipitation alongside temperature can clarify whether the temperature-body mass relationship is expressed consistently across wetter and drier climatic contexts or is modified by a second environmental axis.

Here, we extend previous work on migration as a moderator of Bergmann's rule by analysing more than 10,000 primarily terrestrial bird species under separate breeding- and non-breeding-season climate assignments. This design allows us to ask whether the interspecific temperature-body mass relationship depends on the seasonal climatic exposure assigned to migratory species or is retained despite seasonal movement. We ask (1) whether seasonal temperature is negatively associated with body mass, (2) whether migratory species show a shallower temperature-body mass slope than resident species and whether they differ in average body mass after accounting for seasonal climatic exposure, and (3) whether precipitation modifies the temperature-body mass relationship. If migration weakens the slope, this would support the view that seasonal exposure contributes to the observed Bergmann pattern. If the slope is retained in migratory species, this would suggest that current seasonal exposure alone is insufficient to explain the interspecific pattern.

Materials and methods

This study follows a pre-registered protocol (https://doi.org/10.17605/OSF.IO/DSH2A). All data handling and analyses were conducted in R v. 4.6.0 (R Core Team, 2026), and the full datasets and analysis scripts are archived on Zenodo (https://doi.org/10.5281/zenodo.21687158). The main analytical workflow is summarized below, with full procedural details provided in the Supplementary Methods S1-S4.

The biological comparison was between resident and migratory species. To assess whether this comparison depended on the seasonal climate assigned to migratory species, we created two climate-assignment datasets that differed in the seasonal climate given to migratory species. We then applied the same model structure to each dataset separately. In the breeding-season assignment, resident species were assigned climate from their year-round resident ranges, whereas migratory species were assigned climate from breeding ranges during the breeding-season window. In the non-breeding-season assignment, resident species retained the same year-round climate values, whereas migratory species were assigned climate from non-breeding ranges during the non-breeding-season window. Thus, the two datasets used the same species-level body-mass response and the same resident climate values; they differed only in the seasonal species distribution range and months used to summarize climate for migratory species.

Data and species classification

We obtained adult body mass from AVONET (Tobias et al., 2022). Species distribution polygons and their seasonal range categories, classified as resident, breeding, or non-breeding, were obtained from the *Bird species distribution maps of the world*, Version 2025.2 (BirdLife International & Handbook of the Birds of the World, 2025), accessed on 1 February 2026. Phylogenetic trees were obtained from McTavish et al. (2025) via the *clootl* package *v.0.1.4* (Miller et al., 2026). All data sources were standardized to the BirdLife International taxonomy (HBW and BirdLife Taxonomic Checklist v.10).

We classified species as migratory or resident using the seasonal range categories in the BirdLife distribution polygons. A species was classified as migratory if at least one of its range polygons was designated as breeding or non-breeding. Species whose distributions contained only resident polygons were classified as resident. Species with both resident and season-specific polygons were classified as migratory at the species level because the main comparison asked whether any mapped seasonal movement was associated with the temperature-body mass relationship. Their resident polygons were nevertheless retained when estimating climatic exposure, as described

below. This classification identifies seasonal range movement represented in the BirdLife distribution maps, but does not distinguish partial migration, altitudinal migration, migration distance, or population-level variation in migratory behavior.

We focused primarily on terrestrial and freshwater birds and excluded Procellariiformes and Sphenisciformes since the WorldClim dataset used does not cover marine areas and could not adequately characterize the climatic environments experienced by these predominantly marine orders. Freshwater and coastal waterbirds outside these orders were retained when they could be matched across data sources. We also excluded species that could not be matched across body mass, range, and phylogenetic sources, or for which seasonal climatic exposure could not be summarized under the rules described below.

After these filters, the analytical datasets comprised 10,438 species under the breeding-season climate assignment and 10,431 species under the non-breeding-season climate assignment. Both analytical datasets included the same 8,624 resident species, with climate summarized from their year-round resident ranges. The breeding-season analytical dataset included 1,814 migratory species, and the non-breeding-season analytical dataset included 1,807 migratory species. Of these, 1,805 migratory species had both breeding- and non-breeding-season climate summaries and were used in the within-migrant seasonal-shift analyses. Small differences in migratory sample size between the two analytical datasets resulted from the seasonal-window and overlap-handling rules, which are described in Supplementary Methods S1.2-S1.4. Further details on body-mass data, taxonomic standardisation, phylogenetic matching, species classification, and construction of the analytical datasets are provided in Supplementary Methods S2.1-S2.3.

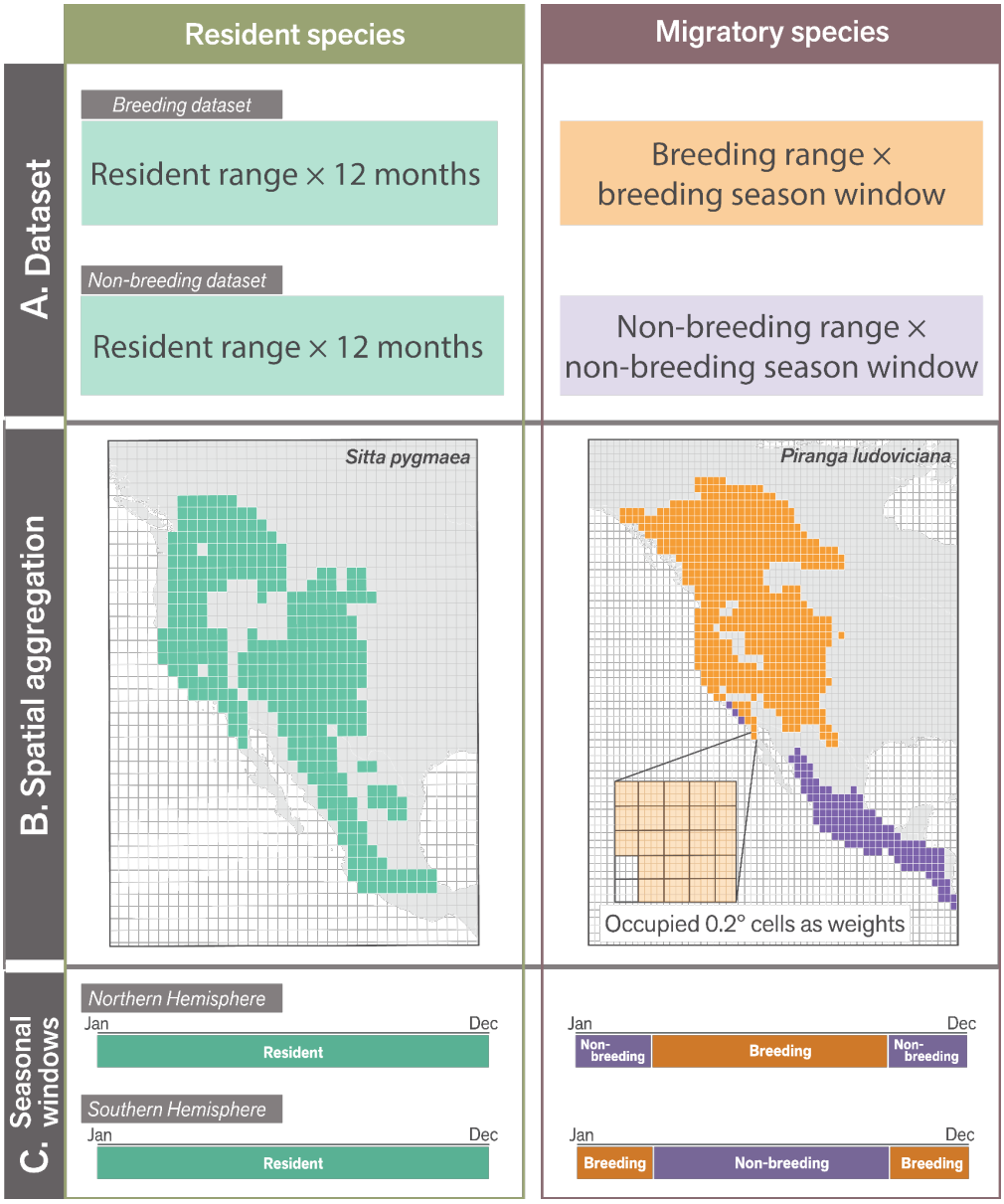

Figure 2. Schematic overview of species-level seasonal climatic exposure assignment. (A) Construction of the breeding-season and non-breeding-season climate-assignment datasets for resident and migratory species. For resident species, both datasets were based on resident range polygons and climate values across all 12 months. For migratory species, the breeding-season dataset was based on breeding range polygons and the corresponding hemisphere-specific breeding-season window, whereas the non-breeding-season dataset was based on non-breeding range polygons and the corresponding non-breeding-season window. (B) Relevant range polygons were rasterized to occupied 0.2° cells. Climate values were aggregated to 1° grid-cell summaries and then combined into species-level summaries using the occupied 0.2° cells as area-based weights. (C) Seasonal windows used for resident and migratory species in the Northern and Southern Hemispheres. For migratory species whose distribution maps also included resident polygons, those polygons were retained and contributed year-round climate values to both climate-assignment datasets.

Seasonal climatic exposure

For each species, we estimated seasonal climatic exposure as a range-area-weighted summary of monthly temperature and precipitation over the range polygons occupied during a specified seasonal window. Climate data came from WorldClim v2.1 (Fick & Hijmans, 2017), and spatial operations on range polygons and raster layers used the *sf v.1.1-1* (Pebesma, 2018; Pebesma & Bivand, 2023) and *terra v.1.9-27* (Hijmans et al., 2026) packages.

The two climate assignments determined which range polygons and months contributed to each species-level climate summary (Figure 2). Under the breeding-season assignment, climate for resident species was summarized from resident ranges across all 12 months, whereas climate for migratory species was summarized from breeding ranges during the breeding-season window. Under the non-breeding-season assignment, climate for resident species was again summarized from resident ranges across all 12 months, whereas climate for migratory species was summarized from non-breeding ranges during the non-breeding-season window. Thus, the two assignments differed only in whether climatic exposure for migratory species was calculated from breeding ranges during the breeding-season window or from non-breeding ranges during the non-breeding-season window.

Some species classified as migratory also contained resident range polygons. For these species, resident polygons contributed year-round climate under both climate assignments, whereas breeding polygons contributed only under the breeding-season assignment, and non-breeding polygons contributed only under the non-breeding-season assignment. When range categories overlapped within the same grid cell, resident range occupancy was given precedence to avoid counting the same occupied area more than once.

Seasonal windows were developed specifically for this study using WorldClim v2.1 monthly mean temperature data. Within each hemisphere, we examined monthly temperature profiles for the latitude bands listed in Table S1 and assigned a common breeding-season window to each band that approximately corresponded to the contiguous months with above-freezing mean temperatures. The remaining months were assigned to the complementary non-breeding-season window. Because above-freezing conditions occurred over fewer months at higher latitudes, the breeding-season windows became shorter toward the poles. These climate-based windows provide an operational approximation of broad seasonal exposure rather than species-specific breeding phenology.

Within each climate assignment, the relevant resident, breeding, or non-breeding range polygons were rasterised to occupied 0.2° cells (Figure 2B). For each occupied 1° grid cell, we first calculated monthly climate values across the occupied 0.2° cells contained within it. We then calculated each species-level climate summary as a weighted mean across its occupied 1° grid cells, where the weight assigned to each 1° cell was the number of occupied 0.2° cells it contained. Thus, 1° cells containing a larger proportion of the species' mapped range contributed more to the species-level climate summary than partially occupied cells.

For temperature, we summarized WorldClim monthly mean temperature within each seasonal window as three metrics: the lowest, average, and highest monthly mean temperature. The average of monthly mean temperature values within the seasonal window was the focal temperature metric, whereas the lowest and highest monthly mean values were examined in alternative candidate models. Mean monthly precipitation was included in all models. Full details of rasterization, range-overlap handling, seasonal-window definitions, and occupied-area weighting are provided in Supplementary Methods S1.1-S1.5.

Statistical analysis

We fitted species-level phylogenetic linear models using the *phylolm* package *v.2.6.5* (Ho et al., 2020; Ho & Ané, 2014), with Pagel's λ used to model phylogenetic non-independence. The response variable was adult body mass, which was natural-log-transformed before analysis. Before model fitting, log body mass and all climatic predictors were z-standardized on a common scale across the two analytical datasets.

The main models compared resident and migratory species separately under the breeding- and non-breeding-season climate assignments. These models tested whether body mass declined with seasonal temperature, whether the temperature-body mass slope differed between migratory and resident species, and whether migratory species differed from resident species in average body mass after accounting for seasonal climate. In these models, predictors were seasonal temperature, precipitation, migratory status, and their interactions, where specified. Resident species were the reference category.

For each climate assignment, we fitted six pre-specified candidate models comparing resident and migratory species. These models used the three seasonal temperature metrics described above, each fitted either as a main-effects model or with all two-way interactions among temperature, precipitation, and migratory status. Under each climate assignment, the model with the lowest AIC

was used to report coefficients. Full candidate-model definitions are provided in Supplementary Methods S3.1-S3.2.

All candidate models were fitted across 50 phylogenetic trees sampled from a pool of 100 trees. We compared models using AIC averaged across the 50 trees to account for phylogenetic uncertainty. Coefficients were pooled across trees using Rubin's rules (Nakagawa & De Villemereuil, 2019) and summarized with Wald-Rubin 95% confidence intervals. Uncertainty in Pagel's λ and in the variance components was estimated by parametric bootstrapping within each tree. Estimates were then pooled across trees on the logit scale for λ and on the log scale for variance components before back-transformation. Group-specific slopes for resident and migratory species were obtained from an equivalent nested re-parameterization. For interpretation, coefficients were converted from the standardized model scale to percentage change in body mass per 1 °C increase in temperature and per 100 mm/month increase in precipitation. Details are provided in Supplementary Methods S3.3-S3.5. Results under the alternative fixed seasonal-window scenario are reported as a sensitivity analysis in Table S8.

Seasonal-shift analyses within migratory species

We conducted two additional analyses restricted to migratory species with both breeding- and non-breeding-season climate summaries. First, we assessed how closely the two seasonal climate summaries corresponded within the same species. For each climate variable, we compared the non-breeding-season value with the breeding-season value and reported the raw Pearson correlation and a phylogenetically corrected slope of the non-breeding-season value on the breeding-season value, estimated under the same Pagel's λ framework. We also summarised the mean seasonal shift in each climate variable as the non-breeding-season value minus the breeding-season value.

Second, we tested whether body mass was associated with the magnitude of seasonal climatic shifts experienced by migratory species. These analyses were restricted to migratory species because resident species were assigned the same year-round climate values under both climate assignments and therefore had no corresponding seasonal shift. For each migratory species, we calculated seasonal temperature shift as non-breeding-season mean temperature minus breeding-season mean temperature, and seasonal precipitation shift as non-breeding-season mean precipitation minus breeding-season mean precipitation. We then fitted phylogenetic models of body mass including breeding-season temperature, breeding-season precipitation, seasonal temperature shift, and seasonal precipitation shift. We also fitted a shift-interaction model that

added the interaction between breeding-season temperature and seasonal temperature shift. These analyses used the same species-level seasonal climatic exposure summaries and phylogenetic modeling framework described in Supplementary Methods S1.5 and S3.1.

Variance-decomposition check

Finally, we conducted a variance-decomposition check to help interpret how much residual body-mass variation remained phylogenetically structured after accounting for the fixed effects. Using the primary model fitted on a single consensus tree rescaled to unit tip height, we partitioned residual body-mass variance into phylogenetically structured, $\sigma^2\lambda$, and non-phylogenetic, $\sigma^2(1 - \lambda)$, components based on Pagel's λ (Freckleton et al., 2002; Pagel, 1999). We then compared nested models with and without the temperature-by-migration interaction, asking whether adding the interaction reduced either component of residual body-mass variation. Full details of the rationale, variance decomposition, and nested comparison are provided in Supplementary Methods S4.1-S4.3.

Pre-registered protocol and amendments

We changed the analytical unit from species-cell observations to species-level observations to align the analysis with the registered interspecific question. In the registered species-cell design, the same species-level body-mass value would have been repeated across all occupied grid cells of a species. This would have created a mismatch between the level of the response variable and the level of climatic exposure, and could have conflated within-species spatial climate variation with between-species climate-body size associations. Aggregating cell-level exposure to species-level summaries aligned the unit of analysis with the interspecific estimand. The underlying seasonal range and climate processing were unchanged: cell-level exposure was still derived from the same BirdLife range polygons and WorldClim layers, then aggregated to the species level before model fitting. Consequently, we used a maximum-likelihood phylogenetic model instead of the originally planned Bayesian model. The biological aims, predictions, taxonomic scope, data sources, and seasonal-exposure framework were unchanged. The rationale for this amendment and its implications for the analytical framework are described in Supplementary Methods S4.4.

Results

Mean monthly temperature was the best-supported temperature metric under both climate assignments. In both cases, the lowest-AIC model included mean monthly temperature, precipitation, migratory status, and all two-way interactions among these predictors (Table S2). Because the two assignments yielded similar estimates of direction, magnitude, and statistical support, we present the breeding-season assignment in the main text and in Figure 3. The corresponding non-breeding-season results are reported in Figure S1 and Tables S3-S5.

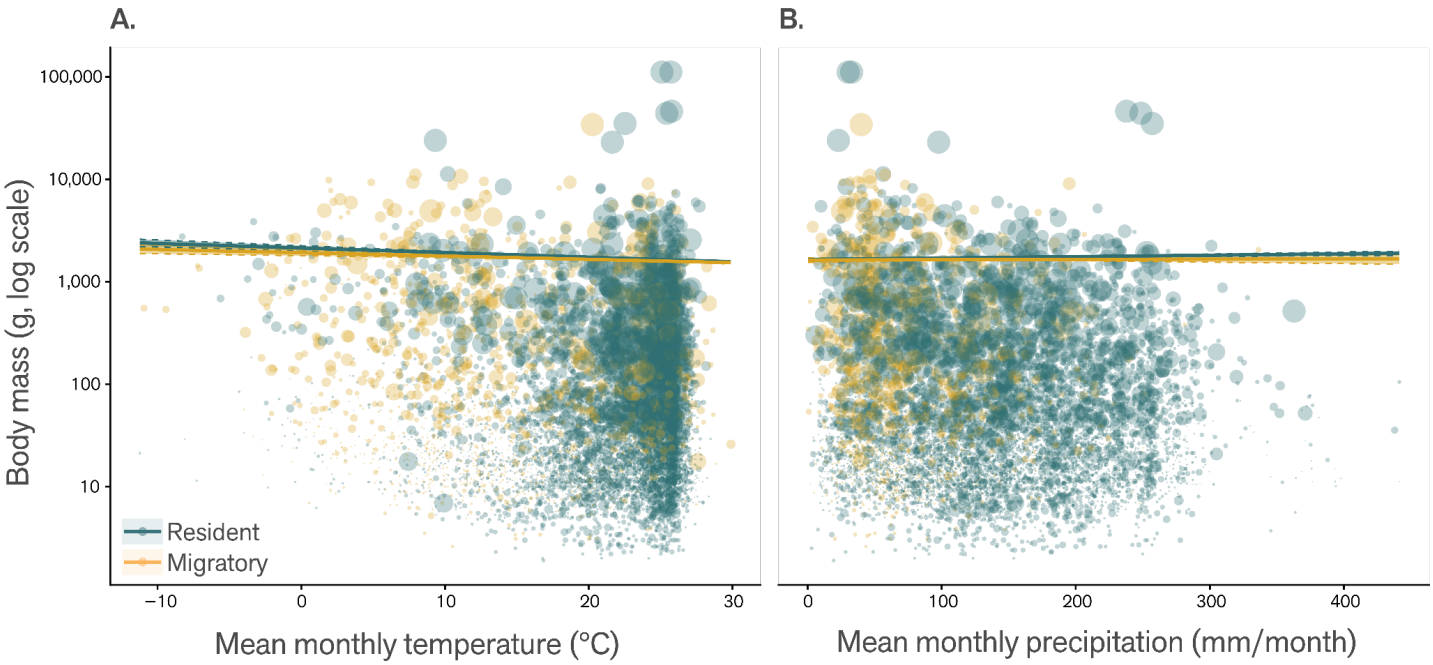

Figure 3. Relationships between body mass and climatic exposure under the breeding-season climate assignment. Panels show mean monthly temperature exposure (A) and mean monthly precipitation exposure (B). Under this assignment, resident species were assigned climatic exposure from resident range polygons across all 12 months. Migratory species were assigned climatic exposure from breeding-range polygons during the breeding-season window; for migratory species that also had resident-range polygons, those resident polygons were retained and contributed year-round climatic exposure. Points show species-level body mass against each climatic predictor on its original scale, with body mass shown on a logarithmic scale. Point size is proportional to each species' phylogenetic weight in the model, so that large-bodied, evolutionarily isolated lineages, which carry most of the independent information in the phylogenetic fit, are emphasized, while species in densely sampled clades are de-emphasized. Solid lines show fitted relationships from the primary phylogenetic linear model for resident and migratory species, with the other climatic predictor held at its species-level mean. Dashed lines and shaded wedges show 95% confidence intervals for the fitted relationships. Colours indicate resident species in green and migratory species in yellow.

Temperature, migration, and body mass

In resident species, each 1 °C higher mean temperature exposure corresponded to an estimated 1.02% lower body mass (β = -0.040, 95% confidence interval [-0.049, -0.030]; Figure 3A; Table S3). In migratory species, each 1 °C higher temperature exposure corresponded to an estimated 0.74% lower body mass (β = -0.029, 95% CI [-0.041, -0.016]; Figure 3A; Table S3). The migrant-resident difference in the temperature-body mass slope was not significant (β = 0.011, 95% CI [-0.002, 0.024]; Table S4). Adding the temperature-by-migration term alone to the corresponding main-effects model also did not improve model support (ΔAIC = 0.90; Table S2). Migratory species differed more clearly from residents in average body mass. When temperature and precipitation were held at their overall species-level means, migratory species were estimated to be 4.57% smaller than resident species (β = -0.030, 95% CI [-0.049, -0.011]; Table S3).

Precipitation

Body mass increased with mean precipitation in resident species, by an estimated 3.18% per 100 mm/month increase in precipitation exposure (β = 0.014, 95% CI [0.008, 0.021]; Figure 3B; Table S3). In migratory species, the corresponding precipitation slope was close to zero, with a 95% CI spanning both negative and positive values (0.63%; β = 0.003, 95% CI [-0.015, 0.021]; Figure 3B; Table S3). The 95% CI for the temperature-by-precipitation interaction narrowly included zero (β = 0.007, 95% CI [-0.00003, 0.014]; Tables S3 and S4), and the precipitation-by-migration interaction also had a confidence interval spanning zero (β = -0.012, 95% CI [-0.031, 0.008]; Table S4).

Phylogenetic structure

After accounting for seasonal climate, migratory status, and their interactions, residual body-mass variation remained strongly phylogenetically structured. Under the breeding-season climate assignment, Pagel's λ was 0.989 (95% CI [0.980, 0.994]; Table S5). The phylogenetic standard deviation was 0.904 (95% CI [0.680, 1.202]), whereas the non-phylogenetic standard deviation was 0.095 (95% CI [0.086, 0.105]) on the standardized scale. The non-phylogenetic component accounted for approximately 1% of the residual variance.

Seasonal-shift analyses within migratory species

The breeding- and non-breeding-season climate summaries were correlated within migratory species. For mean monthly temperature, the Pearson correlation between the two climate summaries was 0.75 (95% CI [0.73, 0.77]), and the phylogenetically corrected slope of the non-

breeding-season climate summary on the breeding-season climate summary was 0.70 (Table S6). For mean monthly precipitation, the Pearson correlation was 0.72 (95% CI [0.70, 0.74]), and the corresponding phylogenetically corrected slope was 0.71 (Table S6).

On average, migratory species experienced warmer temperatures during the non-breeding season than during the breeding season. Mean monthly temperature increased from 14.74 °C to 16.76 °C, giving a mean seasonal shift of +2.03 °C. Coldest-month temperature increased from 4.38 °C to 11.07 °C, giving a mean seasonal shift of +6.68 °C. Mean monthly precipitation changed from 76.98 to 74.04 mm/month, giving a mean seasonal shift of -2.95 mm/month (Table S6). Seasonal shifts were calculated only for migratory species, as resident species had identical climate values under both assignments. The analysis does not compare shifts or climatic extremes between resident and migratory species.

Within migratory species, seasonal temperature shift was associated with body mass. In the within-migrant mean-temperature model, species whose non-breeding ranges were warmer relative to their breeding ranges had lower body mass after accounting for breeding-season temperature and precipitation (β = -0.038, 95% CI [-0.054, -0.023]; Table S7). The coldest-month sensitivity model showed the same pattern, with a larger estimated magnitude (β = -0.057, 95% CI [-0.075, -0.039]; Table S7). Seasonal precipitation shift was not clearly associated with body mass in either model (mean-temperature model: β = 0.003, 95% CI [-0.011, 0.016]; coldest-month model: β = 0.0003, 95% CI [-0.013, 0.013]; Table S7).

Discussion

Seasonal migration did not clearly weaken the interspecific avian Bergmann's rule pattern. Body mass declined with increasing seasonal temperature in both resident and migratory species, and this negative temperature-body mass relationship was retained under both the breeding- and non-breeding-season climate assignments. Although the estimated slope was slightly shallower in migratory species, the migrant-resident difference in slope was small and weak, and the temperature-by-migration term did not improve model support when added on its own. Precipitation provided a secondary climatic context: body mass tended to increase with precipitation in resident species, and there was weak support that precipitation modified the temperature-body mass association. Yet, precipitation did not alter the main conclusion that migratory species retained a negative temperature-body mass relationship. Thus, precipitation should not be interpreted as an alternative explanation for the persistence of the temperature-body mass relationship, but as a variable that captures broader environmental conditions associated with

that pattern. Precipitation is unlikely to represent a single mechanism, because it can covary with water availability, productivity, habitat structure, and resource availability, each of which may influence body size through different pathways (Nwaogu et al., 2018; Ongman et al., 2026; Yom-Tov & Geffen, 2011; Watson & Kerr, 2025).

Migration was associated more clearly with average body size than with a flattening of the temperature-body mass relationship. Previous studies have reached different conclusions about whether migratory birds show weaker or stronger conformity to Bergmann's rule. A worldwide review of intraspecific patterns and a regional interspecific analysis both suggested weaker conformity among migratory than sedentary birds, whereas a global interspecific analysis found stronger conformity among migratory species (He et al., 2023; Mainwaring & Street, 2021; Meiri & Dayan, 2003). These findings are not directly comparable because they differ in analytical scale, the level of biological variation examined, and the climatic or geographic predictors used. Our analysis distinguishes two conceptually separate quantities: the temperature-body mass slope and the average body-mass difference between migratory and resident species. Migratory species retained a negative temperature-body mass relationship but were smaller than resident species after accounting for seasonal climatic exposure. The smaller average size of migratory species is consistent with energetic and aerodynamic constraints on sustained flight, annual-cycle scheduling, and broader life-history differences between migratory and resident birds (Alerstam et al., 2003; Hedenström, 2008; Soriano-Redondo et al., 2020).

Among migratory species, those whose non-breeding-season temperatures were warmer relative to their breeding-season temperatures also had lower body mass. This seasonal contrast is broadly consistent with Dufour et al. (2020), who found that long-distance migrants tended to occupy warmer thermal niches during the non-breeding season than during the breeding season. Our result suggests that the seasonal climate experienced by migratory species is relevant to body-size variation, although the underlying mechanism remains unclear. Nevertheless, the retention of the Bergmann pattern in migratory species suggests that current seasonal exposure alone is unlikely to explain the temperature-body mass relationship. If body size remains associated with climate even when migratory species alter their seasonal exposure, the interspecific pattern may reflect a broader historical link among body size, climatic niches, and migration.

One possibility is that climate-associated body-size variation predates the present migratory regimes of at least some avian lineages. Under this Bergmann-first scenario, an association between colder climatic occupation and larger body size evolved first, and subsequent changes in migratory behaviour altered annual-cycle exposure without erasing that older association. The

temporal sequence may differ among clades, however, since migratory behaviour has arisen and been lost repeatedly across avian evolution (Dufour et al., 2020). This Bergmann-first scenario is consistent with phylogenetic niche conservatism and temperate-origin scenarios for the evolution of migration (Crisp & Cook, 2012; Peterson et al., 1999; Wiens & Graham, 2005; Winger et al., 2014). A second possibility is evolutionary lag or inertia. In this scenario, the temperature-body mass association also predates the current seasonal exposure of migratory species, but the emphasis is on delayed trait tracking: seasonal migration or range shifts changed the climates experienced across the annual cycle, while body size retained an inherited association because its evolution was constrained by stabilizing selection, developmental architecture, or correlated ecological traits (Blomberg et al., 2003; Hansen, 1997; Revell et al., 2008). A third possibility is that there was no simple temporal sequence, because body size, climatic niche, geographic range, and migration evolved together as lineages encountered and persisted in seasonal environments (Cox, 1985; Winger et al., 2019). Together, these results suggest that seasonal climate contributes to avian body-size variation, but that present-day seasonal exposure alone is unlikely to explain the persistence of the interspecific temperature-body mass relationship.

Several limitations qualify these conclusions. First, our seasonal exposure contrast was coarse. Breeding- and non-breeding-season exposure estimates were correlated among migratory species, and migratory species shifted only partially toward milder conditions outside the breeding season. The agreement between the two climate assignments should be interpreted as robustness to a partial change in exposure, rather than as two independent tests of a fully distinct exposure contrast. In addition, climatic exposure was summarised differently for residents and migrants within each assignment: annual exposure for residents, but season-specific exposure for migrants. This difference follows from the biological contrast we aimed to test, but it also means that resident and migratory species were not assigned climatic exposure in exactly the same way. Second, the temperature-by-migration interaction was difficult to resolve. High phylogenetic dependence in body mass and the binary treatment of migration limited the independent information available for estimating migrant-resident differences in slope. The confidence interval for the slope difference was compatible with both negligible and modest migrant-resident differences, and should not be interpreted as evidence that resident and migratory species have identical slopes. Migration was also treated as a binary species-level category, which cannot capture partial migration, altitudinal migration, migration distance, population-level variation in migratory behaviour, migratory routes, stopover conditions, or the climates experienced by individual birds. Finally, each species was represented by an average adult body-mass estimate, whereas climatic exposure was summarised from long-term climate data over species' seasonal

ranges. The body-mass and climate data were therefore not temporally matched, which may have introduced additional variation into the estimated climate-body mass relationships. A more direct test would combine migration distance, annual-cycle timing, tracking data, population-level body-size data, and temporally matched morphological and climate data to assess whether migration modifies body-size responses at finer spatial, temporal, and biological scales than global range-level summaries can capture.

Conclusion

We found that migratory species retained a negative temperature-body mass relationship under both breeding- and non-breeding-season climate assignments, but differed from residents more clearly in average body size. Migratory species were smaller than residents after accounting for seasonal climatic exposure, and within the migratory group, body mass was lower in species experiencing larger seasonal temperature shifts. Precipitation provided a secondary climatic context, but did not alter the main conclusion. Thus, seasonal climate helps define the relevant ecological context, but the persistence of the temperature-body mass relationship in migratory species indicates that this pattern is not solely attributable to current seasonal exposure. This distinction is important in the context of climate change, because spatial trait-climate associations are often used to infer how traits may respond to warming (Radchuk et al., 2019; Urban et al., 2024). Our results suggest that such inferences should be made cautiously: even when body size is associated with current climate, the pattern may also reflect seasonal exposure, shared evolutionary history, historical biogeography, and life history.

References

Alerstam, T., Hedenström, A., & Åkesson, S. (2003). Long-distance migration: evolution and determinants. *Oikos*, *103*(2), 247–260.

Allen, J. A. (1877). The influence of physical conditions in the genesis of species. *Radical Review*, *1*, 108–140.

Baldwin, J. W., Garcia-Porta, J., & Botero, C. A. (2023). Complementarity in Allen's and Bergmann's rules among birds. *Nature Communications*, *14*(1), 4240.

Bergmann, C. (1847). *Über die Verhältnisse der Wärmeökonomie der Thiere zu ihrer Größe*. https://archive.org/details/bub_gb_EHo-AAAAcAAJ

BirdLife International and Handbook of the Birds of the World. (2025). *Bird species distribution maps of the world* (Version 2025.2). Available at http://datazone.birdlife.org/species/requestdis.

Blackburn, T. M., Gaston, K. J., & Loder, N. (1999). Geographic gradients in body size: a clarification of Bergmann's rule. *Diversity & Distributions*, *5*(4), 165–174.

Blomberg, S. P., Garland, T., Jr, & Ives, A. R. (2003). Testing for phylogenetic signal in comparative data: behavioral traits are more labile. *Evolution*, *57*(4), 717–745.

Cox, G. W. (1985). The evolution of avian migration systems between temperate and tropical regions of the new world. *The American Naturalist*, *126*(4), 451–474.

Crisp, M. D., & Cook, L. G. (2012). Phylogenetic niche conservatism: what are the underlying evolutionary and ecological causes? *The New Phytologist*, *196*(3), 681–694.

Delhey, K. (2019). A review of Gloger's rule, an ecogeographical rule of colour: definitions, interpretations and evidence. *Biological Reviews of the Cambridge Philosophical Society*, *94*(4), 1294–1316.

Dufour, P., Descamps, S., Chantepie, S., Renaud, J., Guéguen, M., Schiffers, K., Thuiller, W., & Lavergne, S. (2020). Reconstructing the geographic and climatic origins of long-distance bird migrations. *Journal of Biogeography*, *47*(1), 155–166.

Eyres, A., Böhning-Gaese, K., Orme, C. D. L., Rahbek, C., & Fritz, S. A. (2020). A tale of two seasons: The link between seasonal migration and climatic niches in passerine birds. *Ecology and Evolution*, *10*(21), 11983–11997.

Fick, S. E., & Hijmans, R. J. (2017). WorldClim 2: new 1-km spatial resolution climate surfaces for global land areas. *International Journal of Climatology: A Journal of the Royal Meteorological Society*, *37*(12), 4302–4315.

Freckleton, R. P., Harvey, P. H., & Pagel, M. (2002). Phylogenetic analysis and comparative data: a test and review of evidence. *The American Naturalist*, *160*(6), 712–726.

Fröhlich, A., Kotowska, D., Martyka, R., & Symonds, M. R. E. (2023). Allometry reveals trade-offs between Bergmann's and Allen's rules, and different avian adaptive strategies for thermoregulation. *Nature Communications*, *14*(1), 1101.

Hansen, T. F. (1997). Stabilizing selection and the comparative analysis of adaptation. *Evolution, 51*(5), 1341–1351.

He, J., Tu, J., Yu, J., & Jiang, H. (2023). A global assessment of Bergmann's rule in mammals and birds. *Global Change Biology*, *29*(18), 5199–5210.

Hedenström, A. (2008). Adaptations to migration in birds: behavioural strategies, morphology and scaling effects. *Philosophical Transactions of the Royal Society of London. Series B, Biological Sciences*, *363*(1490), 287–299.

Hijmans, R. J., Brown, A., & Barbosa, M. (2026). *terra: R package for spatial data handling*. https://github.com/rspatial/terra

Ho, T., & Ané, C. (2014). A linear-time algorithm for Gaussian and non-Gaussian trait evolution models. *Systematic Biology*, *63*(3), 397–408.

Ho, T., Ané, C., Lachlan, R., Tarpinian, K., Feldman, R., Yu, Q., Bijl, W. van der, Maspons, J., & Vos, R. (2020). *phylolm: Phylogenetic Linear Regression* (2.6.5) [Computer software]. https://CRAN.R-project.org/package=phylolm

Mainwaring, M. C., & Street, S. E. (2021). Conformity to Bergmann's rule in birds depends on nest design and migration. *Ecology and Evolution*, *11*(19), 13118–13127.

McTavish, E. J., Gerbracht, J. A., Holder, M. T., Iliff, M. J., Lepage, D., Rasmussen, P. C., Redelings, B. D., Reyes, L. L. S., & Miller, E. T. (2025). A complete and dynamic tree of birds. *Proceedings of the National Academy of Sciences*, *122*(18), e2409658122.

Meiri, S., & Dayan, T. (2003). On the validity of Bergmann's rule: On the validity of Bergmann's rule. *Journal of Biogeography*, *30*(3), 331–351.

Miller, E., Sánchez Reyes, L., & McTavish, E. J. (2026). clootl: an R package for accessing and manipulating a complete, versioned avian phylogeny. In *bioRxiv* (p. 2026.04.23.720449). bioRxiv. https://doi.org/10.64898/2026.04.23.720449

Millien, V., Kathleen Lyons, S., Olson, L., Smith, F. A., Wilson, A. B., & Yom-Tov, Y. (2006). Ecotypic variation in the context of global climate change: revisiting the rules. *Ecology Letters*, *9*(7), 853–869.

Nakagawa, S., & De Villemereuil, P. (2019). A General Method for Simultaneously Accounting for Phylogenetic and Species Sampling Uncertainty via Rubin's Rules in Comparative Analysis. *Systematic Biology*, *68*(4), 632–641.

Nwaogu, C. J., Tieleman, B. I., Bitrus, K., & Cresswell, W. (2018). Temperature and aridity determine body size conformity to Bergmann's rule independent of latitudinal differences in a tropical environment. *Journal of Ornithology*, *159*(4), 1053–1062.

Olson, V. A., Davies, R. G., Orme, C. D. L., Thomas, G. H., Meiri, S., Blackburn, T. M., Gaston, K. J., Owens, I. P. F., & Bennett, P. M. (2009). Global biogeography and ecology of body size in birds. *Ecology Letters*, *12*(3), 249–259.

Ongman, K. M., Lundblad, C. G., & Conway, C. J. (2026). Bergmann's rule: Why does body size increase with latitude? *Functional Ecology*, *40*(4), 830–843.

Oskyrko, O., Liu, J., & Du, W. (2026). Is Bergmann's rule valid for terrestrial vertebrates? *Ecology*, *107*(2), e70324.

Pagel, M. (1999). Inferring the historical patterns of biological evolution. *Nature*, *401*(6756), 877–

884.

Pebesma, E. (2018). Simple features for R: Standardized support for spatial vector data. *The R Journal*, *10*(1), 439.

Pebesma, E., & Bivand, R. (2023). *Spatial Data Science: With Applications in R*. Chapman and Hall/CRC.

Peterson, A. T., Soberón, J., & Sánchez-Cordero, V. (1999). Conservatism of ecological niches in evolutionary time. *Science, 285*(5431), 1265–1267.

R Core Team. (2026). *R: A Language and Environment for Statistical Computing* (4.6.0) [Computer software]. https://doi.org/10.32614/R.manuals

Radchuk, V., Reed, T., Teplitsky, C., van de Pol, M., Charmantier, A., Hassall, C., Adamík, P., Adriaensen, F., Ahola, M. P., Arcese, P., Miguel Avilés, J., Balbontin, J., Berg, K. S., Borras, A., Burthe, S., Clobert, J., Dehnhard, N., de Lope, F., Dhondt, A. A., … Kramer-Schadt, S. (2019). Adaptive responses of animals to climate change are most likely insufficient. *Nature Communications*, *10*(1), 3109.

Revell, L. J., Harmon, L. J., & Collar, D. C. (2008). Phylogenetic signal, evolutionary process, and rate. *Systematic Biology*, *57*(4), 591–601.

Salewski, V., & Watt, C. (2017). Bergmann's rule: a biophysiological rule examined in birds. *Oikos*, *126*(2). https://doi.org/10.1111/oik.03698

Somveille, M., Manica, A., Butchart, S. H. M., & Rodrigues, A. S. L. (2013). Mapping global diversity patterns for migratory birds. *PloS One*, *8*(8), e70907.

Somveille, M., Manica, A., & Rodrigues, A. S. L. (2019). Where the wild birds go: explaining the differences in migratory destinations across terrestrial bird species. *Ecography*, *42*(2), 225–236.

Soriano-Redondo, A., Gutiérrez, J. S., Hodgson, D., & Bearhop, S. (2020). Migrant birds and mammals live faster than residents. *Nature Communications*, *11*(1), 5719.

Tobias, J. A., Sheard, C., Pigot, A. L., Devenish, A. J. M., Yang, J., Sayol, F., Neate-Clegg, M. H. C., Alioravainen, N., Weeks, T. L., Barber, R. A., Walkden, P. A., MacGregor, H. E. A., Jones, S. E. I., Vincent, C., Phillips, A. G., Marples, N. M., Montaño-Centellas, F. A., Leandro-Silva, V., Claramunt, S., … Schleuning, M. (2022). AVONET: morphological, ecological and geographical data for all birds. *Ecology Letters*, *25*(3), 581–597.

Urban, M. C., Swaegers, J., Stoks, R., Snook, R. R., Otto, S. P., Noble, D. W. A., Moiron, M., Hällfors, M. H., Gómez-Llano, M., Fior, S., Cote, J., Charmantier, A., Bestion, E., Berger, D., Baur, J., Alexander, J. M., Saastamoinen, M., Edelsparre, A. H., & Teplitsky, C. (2024). When and how can we predict adaptive responses to climate change? *Evolution Letters*, *8*(1), 172–187.

Watson, M. J., & Kerr, J. T. (2025). Climate-driven body size changes in birds and mammals reveal environmental tolerance limits. *Global Change Biology*, *31*(5), e70241.

Wiens, J. J., & Graham, C. H. (2005). Niche conservatism: Integrating evolution, ecology, and conservation biology. *Annual Review of Ecology, Evolution, and Systematics*, *36*(1), 519–539.

Winger, B. M., Auteri, G. G., Pegan, T. M., & Weeks, B. C. (2019). A long winter for the Red Queen: rethinking the evolution of seasonal migration. *Biological Reviews of the Cambridge*

Philosophical Society, *94*(3), 737–752.

Winger, B. M., Barker, F. K., & Ree, R. H. (2014). Temperate origins of long-distance seasonal migration in New World songbirds. *Proceedings of the National Academy of Sciences of the United States of America*, *111*(33), 12115–12120.

Yom-Tov, Y., & Geffen, E. (2011). Recent spatial and temporal changes in body size of terrestrial vertebrates: probable causes and pitfalls. *Biological Reviews of the Cambridge Philosophical Society*, *86*(2), 531–541.

Supplementary materials

Supplementary Methods S1. Detailed protocol for assigning seasonal climatic exposure

This section provides the detailed protocol used to assign seasonally explicit climatic exposure to each species. The protocol follows the pre-registered seasonal-exposure framework, with one amendment: cell-level climatic exposure was aggregated to species-level summaries before model fitting, because the response variable, adult body mass, was available at the species level.

S1.1 Spatial domain and rasterisation

Geographic range polygons were obtained from BirdLife International Datazone (accessed on 1 February 2026) and rasterised separately for each species and seasonality category.
Vector and raster operations used the *sf* v.1.1-1 (Pebesma, 2018; Pebesma & Bivand, 2023) and t*erra* v.1.9-27 (Hijmans et al., 2026) packages. We used native resident, breeding, and non-breeding range categories to define the seasonal spatial domains. Introduced, reintroduced, and passage areas were excluded.

Range polygons were rasterised to a common 0.2° analysis grid. These fine-scale occupied cells were then aggregated to 1° cells as an intermediate processing step for constructing species-level climatic exposure summaries. The 1° aggregation reduced the number of spatial units by approximately 25-fold while retaining information on the spatial distribution of occupied range area. For reference, 1° corresponds to approximately 111 km in latitude, although the east-west distance represented by 1° longitude decreases with latitude.

Hemisphere was assigned at the 0.2° cell level based on latitude. Cells with latitude ≥ 0 were assigned to the Northern Hemisphere, and cells with latitude < 0 were assigned to the Southern Hemisphere.

S1.2 Seasonal time windows

The primary analyses used a variable temporal scenario in which breeding and non-breeding windows varied among latitude bands within each hemisphere. These windows were developed specifically for this study using WorldClim v2.1 monthly mean temperature data. For each latitude band listed in Table S1, we examined the monthly temperature profile and identified an approximate contiguous period with above-freezing mean temperatures. This period was assigned as the common breeding-season window for records within that latitude band, and the remaining

months were assigned as the complementary non-breeding-season window. This procedure resulted in shorter breeding-season windows at higher latitudes, where above-freezing conditions occurred over fewer months.

We also retained an alternative fixed temporal scenario as a sensitivity analysis. In this scenario, breeding and non-breeding windows were constant within each hemisphere. Results under this scenario are reported in Table S8. Resident records were assigned the annual window, that is, all 12 months, under both temporal scenarios. The month sets used under the primary variable temporal scenario and the alternative fixed temporal scenario are reported in Supplementary Table S1.

Monthly climatic data were obtained from WorldClim v2.1 (Fick & Hijmans, 2017), which represents long-term climatic averages for 1970 to 2000. For temperature, we used monthly mean temperature values. Within each assigned seasonal window, we derived three alternative temperature summaries: the lowest, average, and highest monthly mean temperatures. These summaries describe the coldest, average, and warmest monthly mean conditions within the seasonal window, rather than the monthly minimum or maximum air temperature. The average monthly mean temperature was the focal metric in the main text, whereas the lowest and highest monthly mean temperature summaries were examined in alternative candidate models. For precipitation, we calculated mean monthly precipitation across the assigned monthly window and included this precipitation summary in all candidate models.

S1.3 Overlap-handling rules

BirdLife International range polygons may assign multiple seasonality categories to the same species and grid cell. For example, a species-cell may contain resident and breeding records, or breeding and non-breeding records. Overlap resolution was performed at the species × 1° cell level after climate filtering, using the following pre-specified rules.

Resident precedence: If at least one resident record was present within a species and 1° cell, that species-cell was classified as resident, regardless of whether breeding and/or non-breeding records were also present.

Breeding and non-breeding overlap without resident: If resident records were absent but both breeding and non-breeding records were present within the same species and 1° cell, the species-cell was classified as an overlapping breeding and non-breeding cell. These cells were

assigned according to the focal seasonal model set. They were treated as breeding cells in the breeding-season model set and as non-breeding cells in the non-breeding-season model set.

Breeding only: If breeding records were present but resident and non-breeding records were absent, the species-cell was classified as breeding.

Non-breeding only: If non-breeding records were present but resident and breeding records were absent, the species-cell was classified as non-breeding.

These rules were designed to keep the seasonal classification deterministic and reproducible. Resident records were given precedence because they indicate year-round occupancy of the cell. Breeding and non-breeding overlap was retained only when resident records were absent, and such cells were resolved according to the focal seasonal model set.

S1.4 Species classification and seasonal model sets

Species-level migratory status was assigned from the original BirdLife International seasonality categories before cell-level overlap resolution. Species with any range polygon categorised as breeding or non-breeding were classified as migratory, whereas species represented only by resident range polygons were classified as resident.

We constructed two seasonal model sets. In the breeding-season model set, resident species contributed annual climatic exposure from resident cells, whereas migratory species contributed breeding-season exposure from breeding cells, including overlapping breeding and non-breeding cells resolved as breeding. In the non-breeding-season model set, resident species again contributed annual climatic exposure from resident cells, whereas migratory species contributed non-breeding-season exposure from non-breeding cells, including overlapping breeding and non-breeding cells resolved as non-breeding.

This structure allowed residents and migrants to be compared within the same seasonal model sets while assigning climatic exposure according to each group's range use. Resident species were represented by their year-round resident range in both seasonal model sets. Migratory species were represented by their breeding range in the breeding-season model set and by their non-breeding range in the non-breeding-season model set.

S1.5 Aggregation to species-level climatic exposure summaries

Before model fitting, cell-level climatic exposure values were aggregated to species-level summaries. Aggregation was performed separately for each species, seasonal climate dataset, temporal scenario, and temperature metric.

For each species and seasonal climate dataset, aggregation was based on the retained occupied 1° cells after applying the seasonal-window and overlap-handling rules described above. Species-level climatic exposure was calculated as a weighted mean across retained 1° cells, using the number of contributing occupied 0.2° cells within each 1° cell as weights. Thus, 1° cells representing a larger underlying occupied range area contributed proportionally more to the species-level climatic exposure estimate.

This weighting was intended to approximate climatic exposure across the occupied range area while keeping the final statistical analysis at the species level. For each species and seasonal climate dataset, temperature summaries were calculated separately for the lowest, average, and highest monthly mean temperature metrics. Precipitation was represented as mean monthly precipitation.

Supplementary Methods S2. Species matching, phylogeny, and analytical datasets

S2.1 Body mass data and taxonomic standardisation

Adult body mass data were obtained from AVONET and treated as species-level estimates of adult body size. Body mass was natural-log transformed before analysis. Taxonomic names were harmonized across the body mass, geographic range, and phylogenetic data sources before the analytical datasets were assembled. Because climatic exposure was derived from BirdLife International range polygons, the HBW and BirdLife Taxonomic Checklist v10 served as the reference taxonomy. Body mass and phylogenetic records were first matched automatically to this taxonomy. Records that could not be matched automatically were then reviewed manually against Avibase (https://avibase.bsc-eoc.org/avibase.jsp). This manual review involved 1,230 of the 10,970 species and primarily addressed recent changes in generic classification. Original and resolved taxonomic keys are archived with the data, providing a traceable record of each manual decision. Species without a unique match across the body mass, range, and phylogenetic data after this procedure were excluded from the final analytical datasets.

We focused on extant, primarily terrestrial bird species. Predominantly marine species were excluded because their ecology and the selective pressures shaping body-size variation may differ

from those of primarily terrestrial birds. Specifically, species in Procellariiformes and Sphenisciformes were excluded. After excluding these species and species that could not be matched across data sources, the final analytical datasets comprised 10,438 species in the breeding-season set and 10,431 species in the non-breeding-season set, of which 8,624 were resident and 1,814 and 1,807 were migratory in the breeding- and non-breeding-season sets, respectively. Of these, 1,805 migratory species had valid exposure summaries in both seasonal sets and were used in the within-migrant analyses. Nine migratory species occurred in the breeding-season set, but not the non-breeding-season set, and two occurred in the non-breeding-season set but not the breeding-season set, after applying the seasonal-window and overlap-handling rules.

S2.2 Phylogenetic data

To account for shared evolutionary history and phylogenetic uncertainty, we used avian phylogenetic trees from McTavish et al. (McTavish et al., 2025), obtained through the *clootl* package v.0.1.4 (Miller et al., 2026). Trees were pruned to match the final species set in each seasonal model dataset.

For the comparative analyses, we generated an initial pool of 100 trees and reproducibly sampled 50 trees from this pool. Each candidate model was fitted separately across these 50 trees. This procedure allowed fixed effects, model support, and phylogenetic parameters to reflect both statistical uncertainty within each fitted model and phylogenetic uncertainty across alternative trees.

S2.3 Analytical unit and species-level datasets

The final analytical unit was the species. For each seasonal climate dataset, each species contributed a single species-level record if it had valid climatic exposure, body mass, and phylogenetic information. The breeding-season and non-breeding-season climate datasets were analysed separately, using the same body-mass response but different seasonal climatic exposure summaries for migratory species. This species-level structure differs from the originally registered species-cell analytical unit; the rationale for this amendment is described in Supplementary Methods S4.4.

Supplementary Methods S3. Phylogenetic comparative models and uncertainty propagation

S3.1 Model structure

We fitted species-level phylogenetic linear models using the *phylolm* package *v.2.6.5*, with Pagel's λ used to model phylogenetic non-independence among species. The response variable was standardized log-transformed adult body mass. The explanatory variables were species-level temperature exposure, species-level precipitation exposure, and species-level migratory status. Migratory status was coded as a two-level factor, with resident species as the reference category.

Models were fitted separately for the breeding-season and non-breeding-season climatic exposure datasets. Continuous predictors were centred and standardized before model fitting. For each temporal scenario, we used common species-level scaling constants across the breeding-season and non-breeding-season datasets. This allowed coefficients from the two seasonal model sets to be compared on a common standardized scale.

S3.2 Candidate model set

For each seasonal model set, we compared six pre-specified candidate models. Three models included the main effects of temperature, precipitation, and migratory status. These models differed only in the temperature metric used: lowest, average, or highest monthly mean temperature within the assigned seasonal window.

The other three models used the same three temperature metrics but additionally included all two-way interactions among temperature, precipitation, and migratory status. Thus, the interaction models included the temperature × precipitation interaction, the temperature × migratory status interaction, and the precipitation × migratory status interaction.

The main-effects model can be written as:

$$y_i = \beta_0 + \beta_T T_i + \beta_P P_i + \beta_M M_i + e_i,$$

and the interaction model can be written as:

$$y_i = \beta_0 + \beta_T T_i + \beta_P P_i + \beta_M M_i + \beta_{TP}(T_i P_i) + \beta_{TM}(T_i M_i) + \beta_{PM}(P_i M_i) + e_i,$$

where y_i is the standardized log-transformed body mass of species i, T_i is species-level seasonal temperature exposure, P_i is species-level seasonal precipitation exposure, and M_i indicates migratory status. In the phylogenetic models, the residual covariance structure was modified by Pagel's λ according to the phylogenetic correlation matrix.

Each candidate model was fitted across the 50 phylogenetic trees using maximum likelihood. Model support was evaluated using AIC within each tree, and AIC summaries were then aggregated across the 50 trees. Model selection was based on the overall AIC support for each candidate model. Individual interaction terms were interpreted from their pooled coefficient estimates and confidence intervals rather than from model selection alone.

S3.3 Pooling across phylogenetic trees

Fixed-effect estimates were pooled across the 50 phylogenetic trees using Rubin's rules. For fixed effects, we report Rubin-pooled point estimates and Wald-Rubin 95% confidence intervals.

In the standard reference-coded interaction model, the resident slope and the migratory-versus-resident slope difference are estimated directly. The migratory slope, however, is a linear combination of the resident slope and the interaction coefficient. To present group-specific slopes with directly estimated standard errors, we refitted the selected interaction model using an equivalent nested parameterisation in which resident and migratory slopes were estimated as separate coefficients.

This re-parameterisation does not change the fitted values, likelihood, AIC, Pagel's λ, or variance parameters. It only changes the fixed-effect contrasts. We used the nested parameterisation to summarise group-specific temperature and precipitation slopes directly for resident and migratory species.

S3.4 Parametric bootstrap for phylogenetic and variance parameters

To quantify uncertainty in phylogenetic and variance parameters, we used the parametric bootstrap implemented in phylolm for each fitted model on each phylogenetic tree. Bootstrap replicates were used to estimate within-tree uncertainty for Pagel's λ and variance components.

For variance-related parameters, Rubin's rules were applied on transformed scales before back-transformation. Pagel's λ was pooled on the logit scale, and variance parameters were pooled on the log scale. This transformation was used because λ is bounded between 0 and 1, whereas variance parameters are positive and often right-skewed. Back-transformed estimates and confidence intervals are reported on the original scale.

S3.5 Conversion to natural units

To facilitate biological interpretation, selected coefficients were converted from the standardized model scale to natural units. For temperature, we report the estimated percentage change in body mass per 1 °C increase. For precipitation, we report the estimated percentage change in body mass per 100 mm/month increase.

The conversion was performed by first rescaling the standardized coefficient to the chosen natural-unit change in the predictor. The resulting change in standardized log body mass was then converted back to the log-body-mass scale using the standard deviation of log body mass. Finally, the value was exponentiated and expressed as a percentage change in body mass.

For a continuous predictor x, a coefficient beta_x, a natural-unit change Delta x, the standard deviation of the predictor s_x, and the standard deviation of log body mass s_y, the percentage change in body mass was calculated as:

$$100 \times \left[\exp\left(\beta_x \times \frac{\Delta x}{s_x} \times s_y\right) - 1\right].$$

For the migratory-status main effect, which is a binary contrast, the same transformation was applied with the predictor change equal to one unit. For the temperature × precipitation interaction, the interaction coefficient was rescaled to the joint natural-unit change of 10 °C and 100 mm/month before conversion to percentage body-mass change beyond the additive expectation.

Supplementary Methods S4. Focused variance-decomposition check and protocol amendment

S4.1 Rationale for the variance-decomposition check

The primary interaction model tests whether the temperature-body mass slope differs between resident and migratory species. However, because body mass is expected to be strongly phylogenetically structured, a small or uncertain temperature × migration interaction could arise for two different reasons. First, migration may not explain much variation in body mass beyond shared evolutionary history. Second, migration may explain some variation, but that variation may be embedded in the phylogenetic component of the model rather than in the residual, non-phylogenetic component.

To examine this issue, we performed a focused variance-decomposition check for the temperature × migration interaction. This check was not used for primary model selection. Instead, it was used

to assess whether adding the temperature × migration interaction changed the phylogenetic or non-phylogenetic components of modeled body-mass variation.

S4.2 Variance decomposition under Pagel's λ

For this focused check, we fitted the primary Pagel's λ model on a single consensus tree rather than across the full 50-tree set used for confirmatory inference. The consensus tree was rescaled to unit tip height. This rescaling allowed the fitted variance parameter and Pagel's λ to be interpreted as a partition of modeled variance in standardized log body mass.

Under this representation, the modeled variance was partitioned into a phylogenetic component and a non-phylogenetic component:

$$\sigma^2_{\text{phylogenetic}} = \sigma^2\lambda,$$

$$\sigma^2_{\text{non-phylogenetic}} = \sigma^2(1-\lambda).$$

Here, sigma^2 is the fitted variance parameter and lambda is Pagel's λ. Because Pagel's λ is invariant to uniform rescaling of branch lengths, rescaling the consensus tree to unit tip height affects sigma^2 but not λ.

S4.3 Nested comparison of models with and without the temperature × migration interaction

We compared nested models with and without the temperature × migration interaction. The model without the temperature × migration interaction retained the remaining fixed-effect structure needed for the focused comparison. We then asked whether adding the temperature × migration interaction reduced the phylogenetic component, the non-phylogenetic component, or neither. We also recorded the associated change in AIC.

This analysis was intended to answer a narrow question: whether the temperature × migration term explained appreciable variation in body mass beyond the phylogenetic structure already captured by Pagel's λ. So, the results are interpreted as a descriptive variance-decomposition check rather than as an alternative primary inferential model.

S4.4 Amendment to the pre-registered analytical unit

This study follows a pre-registered protocol, with one amendment introduced before model fitting. The original protocol specified a species-cell analytical dataset, with one row per species per

occupied 1° grid cell, and a Bayesian hierarchical model. We amended the analytical unit to species-level observations, with one row per species per seasonal model set.

The reason for this amendment was that the registered biological question concerns interspecific variation in adult body mass. Adult body mass was available as a species-level trait, not as a cell-level or population-level response. In the originally registered species-cell model, the same species-level body-mass value would have been repeated across multiple occupied grid cells for each species. This structure creates a mismatch between the level of the response variable and the level of climatic exposure, and risks conflating within-species spatial variation in climate with between-species associations between climate and body mass.

The amended species-level analysis aligns the statistical unit of analysis with the level of the response variable and with the registered interspecific question. The underlying seasonal range and climate processing remained unchanged. Cell-level climatic exposure was still constructed from the same BirdLife International range polygons and WorldClim monthly climate layers, but it was aggregated to species-level summaries before model fitting.

Following this amendment, the primary inference was carried out using maximum-likelihood phylogenetic linear models in phylolm. This implementation was appropriate because each final model-specific dataset contained one row per species and because phylolm efficiently accommodates Pagel's λ models across multiple phylogenetic trees.

The amendment did not change the biological aims, predictions, focal taxonomic scope, data sources, or seasonally explicit climate-processing framework. The original species-cell model was not retained as a confirmatory analysis because it no longer matched the amended estimand. Any analyses using alternative climatic summaries or temporal scenarios should therefore be interpreted as sensitivity analyses around the species-level comparative framework, not as tests of the original species-cell model.

Supplementary figures and tables

Table S1. Month sets assigned to records under the primary variable temporal scenario and the alternative fixed temporal scenario. The variable scenario allows breeding and non-breeding windows to vary with latitude within each hemisphere to reflect broad geographic shifts in seasonal temperature regimes. Resident records retain all 12 months under both temporal scenarios.

Temporal scenario	Hemisphere	Latitude band	Seasonality	Start month	End month
Fixed	North	0 to 90°	Breeding	3	10
Fixed	North	0 to 90°	Non-breeding	11	2
Fixed	North	0 to 90°	Resident	1	12
Fixed	South	0 to 90°	Breeding	9	4
Fixed	South	0 to 90°	Non-breeding	5	8
Fixed	South	0 to 90°	Resident	1	12
Variable	North	0 to 50°	Breeding	3	10
Variable	North	50 to 70°	Breeding	4	9
Variable	North	70 to 90°	Breeding	5	8
Variable	North	0 to 50°	Non-breeding	11	2
Variable	North	50 to 70°	Non-breeding	10	3
Variable	North	70 to 90°	Non-breeding	9	4
Variable	North	0 to 90°	Resident	1	12

Variable	South	0 to -30°	Breeding	9	4
Variable	South	-30 to -60°	Breeding	10	3
Variable	South	-60 to -90°	Breeding	11	2
Variable	South	0 to -30°	Non-breeding	5	8
Variable	South	-30 to -60°	Non-breeding	4	9
Variable	South	-60 to -90°	Non-breeding	3	10
Variable	South	0 to -90°	Resident	1	12

Table S2. AIC model comparison across 50 trees (variable scenario)

Temperature metric: min/mean/max = lowest/average/highest monthly mean temperature within the seasonal window. Interaction = all three two-way interactions present. mean_dAIC and Akaike weight are averaged across trees; best_frequency is the proportion of trees in which the model had the lowest AIC. Values are for the primary variable temporal scenario; the corresponding fixed-scenario values are given in Table S8.

Season	Model	Temp metric	Interactions	mean AIC	mean dAIC	mean Akaike w	% of trees with lowest AIC
BR	M5	mean	yes	125.4	0.05	0.751	0.96
BR	M2	mean	no	128.1	2.71	0.233	0.04
BR	M6	max	yes	139.5	14.18	0.016	0
BR	M3	max	no	149.2	23.83	0	0
BR	M4	min	yes	167.1	41.76	0	0
BR	M1	min	no	174.4	49.06	0	0
NR	M5	mean	yes	121.4	0.01	0.91	0.98
NR	M2	mean	no	126.8	5.38	0.09	0.02
NR	M6	max	yes	143.3	21.92	0	0
NR	M3	max	no	153	31.62	0	0
NR	M4	min	yes	153.7	32.32	0	0
NR	M1	min	no	169.4	48.02	0	0

Table S3. Primary model (M5) effects in natural units (variable scenario). Resident and migratory temperature/precipitation slopes are from the nested re-parameterisation; interaction and migration main-effect terms are from the standard parameterisation. Temperature effects are per +1 °C; precipitation effects per +100 mm month-1; the temperature × precipitation term is the body-mass change beyond the additive expectation for a joint +1 °C and +100 mm month-1; the migration main effect is the migratory-minus-resident difference at the species-level common-mean climate.

Effect	Breeding beta (std) [95% CI]	Breeding % change [95% CI]	Non-breeding beta (std) [95% CI]	Non-breeding % change [95% CI]
Temperature slope (resident), per +1 C	-0.040 [-0.049, -0.030]	-1.02% [-1.27, -0.77]	-0.040 [-0.050, -0.031]	-1.04% [-1.29, -0.79]
Temperature slope (migratory), per +1 C	-0.029 [-0.041, -0.016]	-0.74% [-1.05, -0.43]	-0.029 [-0.041, -0.018]	-0.76% [-1.05, -0.47]
Temperature x Migration (slope difference), per +1 C	0.011 [-0.002, 0.024]	0.29% [-0.05, 0.62]	0.011 [-0.001, 0.023]	0.29% [-0.02, 0.60]
Precipitation slope (resident), per +100 mm/mo	0.014 [0.008, 0.021]	3.18% [1.65, 4.74]	0.014 [0.007, 0.021]	3.08% [1.56, 4.63]
Precipitation slope (migratory), per +100 mm/mo	0.003 [-0.015, 0.021]	0.63% [-3.27, 4.69]	-0.0003 [-0.016, 0.016]	-0.07% [-3.48, 3.46]
Precipitation x Migration (slope difference), per +100 mm/mo	-0.012 [-0.031, 0.008]	-2.47% [-6.46, 1.68]	-0.014 [-0.031, 0.003]	-3.06% [-6.58, 0.59]
Temperature x Precipitation (joint +1 C & +100 mm/mo)	0.007 [-0.00003, 0.014]	0.25% [-0.00, 0.50]	0.007 [0.0005, 0.014]	0.26% [0.02, 0.51]
Migration main effect (migratory vs resident, at mean climate)	-0.030 [-0.049, -0.011]	-4.57% [-7.32, -1.73]	-0.026 [-0.045, -0.007]	-3.93% [-6.67, -1.10]

Table S4. Full fixed-effect coefficients on the standardized scale (variable scenario) mean-temperature model with all two-way interactions (primary). Estimates are Rubin-pooled across 50 trees; brackets are Wald-Rubin 95% CIs. Values are for the primary variable temporal scenario; the corresponding fixed-scenario values are given in Table S8.

Season	Term	beta	SE	95% CI
BR	Intercept	2.339	0.462	[1.433, 3.245]
BR	Temperature	-0.04	0.005	[-0.049, -0.030]
BR	Precipitation	0.014	0.004	[0.008, 0.021]
BR	Migration (migratory vs resident)	-0.03	0.01	[-0.049, -0.011]
BR	Temperature x Precipitation	0.007	0.003	[-0.000, 0.014]
BR	Temperature x Migration	0.011	0.007	[-0.002, 0.024]
BR	Precipitation x Migration	-0.012	0.01	[-0.031, 0.008]
NR	Intercept	2.338	0.462	[1.432, 3.244]
NR	Temperature	-0.04	0.005	[-0.050, -0.031]
NR	Precipitation	0.014	0.004	[0.007, 0.021]
NR	Migration (migratory vs resident)	-0.026	0.01	[-0.045, -0.007]
NR	Temperature x Precipitation	0.007	0.003	[0.000, 0.014]
NR	Temperature x Migration	0.011	0.006	[-0.001, 0.023]
NR	Precipitation x Migration	-0.014	0.009	[-0.031, 0.003]

Table S5. Variance components and Pagel's lambda for the primary model M5 (variable scenario) Lambda and sigma^2 are model parameters; sigma_phylo and sigma_E are derived standard deviations on the standardized scale (sigma_phylo = sqrt(sigma^2·lambda·H), sigma_E = sqrt(sigma^2·(1−lambda)) on the unit-height consensus tree). Brackets are parametric-bootstrap 95% CIs pooled across trees. Values are for the primary variable temporal scenario; the corresponding fixed-scenario values are given in Table S8.

Season	Component	Estimate	95% CI
BR	Pagel's lambda	0.989	[0.980, 0.994]
BR	sigma^2	0.008	[0.007, 0.008]
BR	sigma_phylo	0.904	[0.680, 1.202]
BR	sigma_E	0.095	[0.086, 0.105]
NR	Pagel's lambda	0.989	[0.980, 0.994]
NR	sigma^2	0.008	[0.007, 0.008]
NR	sigma_phylo	0.904	[0.680, 1.203]
NR	sigma_E	0.095	[0.086, 0.104]

Table S6. Breeding vs non-breeding climatic exposure within migratory species (n = 1805). (A) reports the raw Pearson correlation (with 95% CI) and a phylogenetically corrected slope of NR on BR exposure estimated under a Pagel's λ model across 50 trees (median and 2.5–97.5% range across trees), together with the median λ. (B) reports the mean breeding and non-breeding exposure, the mean seasonal shift (NR − BR), and the percentage of species that were milder (temperature) or wetter (precipitation) in the non-breeding season. The variable seasonal scenario is the primary analysis; the fixed scenario is shown as a sensitivity analysis. The two seasonal assignments are strongly correlated, and migrants shift only partially toward milder non-breeding conditions, so the agreement between the seasonal model sets reflects robustness to a partial change in exposure rather than two independent contrasts.

A. Correspondence between breeding- (BR) and non-breeding-season (NR) exposure

Scenario	Climate variable	Pearson r [95% CI]	Phylogenetic slope NR~BR (median [2.5-97.5% across trees])	Pagel's lambda (median)
variable (primary)	Coldest-month temperature	0.65 [0.62, 0.68]	0.59 [0.59, 0.60]	0.86
variable (primary)	Mean temperature	0.75 [0.73, 0.77]	0.70 [0.69, 0.70]	0.81
variable (primary)	Warmest-month temperature	0.76 [0.74, 0.78]	0.72 [0.71, 0.73]	0.68
variable (primary)	Mean precipitation	0.72 [0.70, 0.74]	0.71 [0.71, 0.72]	0.61
fixed (sensitivity)	Coldest-month temperature	0.58 [0.55, 0.61]	0.53 [0.52, 0.54]	0.87
fixed (sensitivity)	Mean temperature	0.72 [0.69, 0.74]	0.68 [0.67, 0.68]	0.81
fixed (sensitivity)	Warmest-month temperature	0.76 [0.74, 0.78]	0.72 [0.71, 0.72]	0.68
fixed (sensitivity)	Mean precipitation	0.72 [0.69, 0.74]	0.71 [0.71, 0.71]	0.61

B. Seasonal shift in exposure (non-breeding minus breeding)

Scenario	Climate variable	Mean BR	Mean NR	Mean shift (NR - BR)	% species milder/wetter in NR
variable (primary)	Coldest-month temperature (C)	4.38	11.07	+6.68	83.3
variable (primary)	Mean temperature (C)	14.74	16.76	+2.03	60.4
variable (primary)	Warmest-month temperature (C)	22.47	22.32	-0.15	40.2
variable (primary)	Mean precipitation (mm/month)	76.98	74.04	-2.95	40.7
fixed (sensitivity)	Coldest-month temperature (C)	2.36	11.07	+8.71	88
fixed (sensitivity)	Mean temperature (C)	13.88	16.69	+2.81	64.2
fixed (sensitivity)	Warmest-month temperature (C)	22.47	22.11	-0.36	38.8
fixed (sensitivity)	Mean precipitation (mm/month)	76.1	74.06	-2.04	41.6

Table S7. Within-migrant phylogenetic regression of standardized log body mass on seasonal climatic exposure and on the seasonal shift in exposure, fitted within migratory species (n = 1805) across 50 trees. (A) Rubin-pooled coefficients (Wald-Rubin 95% CIs) for a shift-main model (breeding temperature and precipitation plus their non-breeding-minus-breeding seasonal shifts) and a shift-interaction model (adding a breeding-temperature × temperature-shift term); intercepts are omitted. (B) Mean change in AIC relative to a base model (breeding climate only). All predictors are standardized (z); mean monthly temperature is the focal metric and coldest-month temperature is a sensitivity analysis. In the shift-main models, the seasonal-shift effect was consistently negative across temperature metrics, with comparable estimates for mean and coldest-month temperature. Adding the breeding-temperature × seasonal-shift interaction changed AIC by approximately one unit or less relative to the corresponding shift-main model (ΔAIC = 0.87 and 1.00, respectively), providing little evidence that the interaction improved model fit. The estimated interaction was sensitive to the seasonal-window definition: its 95% confidence interval overlapped zero under the variable scenario but not under the alternative fixed scenario (Table S8). Because breeding and non-breeding temperatures were correlated at approximately 0.75, the interaction was weakly identified and is not interpreted further.

A. Regression coefficients (standardized scale)

Temperature metric	**Model**	**Term**	**beta [95% CI]**
Mean temperature (focal)	shift-main	Breeding temperature	-0.051 [-0.065, -0.036]
Mean temperature (focal)	shift-main	Seasonal temperature shift (NR-BR)	-0.038 [-0.054, -0.023]
Mean temperature (focal)	shift-main	Breeding precipitation	-0.012 [-0.037, 0.013]
Mean temperature (focal)	shift-main	Seasonal precipitation shift (NR-BR)	0.003 [-0.011, 0.016]
Mean temperature (focal)	shift-interaction	Breeding temperature	-0.045 [-0.061, -0.029]
Mean temperature (focal)	shift-interaction	Seasonal temperature shift (NR-BR)	-0.017 [-0.048, 0.014]
Mean temperature (focal)	shift-interaction	Breeding precipitation	-0.013 [-0.038, 0.012]
Mean temperature (focal)	shift-interaction	Seasonal precipitation shift (NR-BR)	0.003 [-0.011, 0.016]
Mean temperature (focal)	shift-interaction	Breeding temperature x seasonal shift	0.010 [-0.002, 0.023]
Coldest-month temperature (sensitivity)	shift-main	Breeding temperature	-0.065 [-0.082, -0.049]
Coldest-month temperature (sensitivity)	shift-main	Seasonal temperature shift (NR-BR)	-0.057 [-0.075, -0.039]
Coldest-month temperature (sensitivity)	shift-main	Breeding precipitation	-0.015 [-0.040, 0.011]
Coldest-month temperature (sensitivity)	shift-main	Seasonal precipitation shift (NR-BR)	0.000 [-0.013, 0.013]
Coldest-month temperature (sensitivity)	shift-interaction	Breeding temperature	-0.057 [-0.076, -0.037]
Coldest-month temperature (sensitivity)	shift-interaction	Seasonal temperature shift (NR-BR)	-0.029 [-0.068, 0.010]
Coldest-month temperature (sensitivity)	shift-interaction	Breeding precipitation	-0.014 [-0.040, 0.011]
Coldest-month temperature (sensitivity)	shift-interaction	Seasonal precipitation shift (NR-BR)	0.002 [-0.011, 0.015]

Coldest-month temperature (sensitivity)	shift-interaction	Breeding temperature x seasonal shift	0.013 [-0.003, 0.028]

B. Model comparison (mean dAIC relative to the base model; more negative = better fit)

Temperature metric	Model	Terms	mean dAIC vs base
Mean temperature (focal)	base	breeding temp + breeding precip	0
Mean temperature (focal)	shift-main	+ seasonal temp & precip shift	-21.1
Mean temperature (focal)	shift-interaction	+ breeding temp x shift	-22
Coldest-month temperature (sensitivity)	base	breeding temp + breeding precip	0
Coldest-month temperature (sensitivity)	shift-main	+ seasonal temp & precip shift	-39.2
Coldest-month temperature (sensitivity)	shift-interaction	+ breeding temp x shift	-40.2

Table S8. Sensitivity of the primary results to the definition of the seasonal windows. The variable temporal scenario is the primary, pre-registered analysis, in which breeding and non-breeding windows shorten toward the poles; the fixed scenario applies the same months at all latitudes within a hemisphere (Table S1). All estimates are Rubin-pooled across the same 50 phylogenetic trees, with Wald-Rubin 95% confidence intervals; the two scenarios differ only in which months contribute to each species' climatic exposure. (A) AIC model comparison across the six candidate models. (B) Standardised fixed-effect coefficients. (C) Variance components and Pagel's λ. (D) Within-migrant seasonal-shift models (n = 1,805). Three results differ between scenarios and are noted here. First, in the breeding season the best-supported model under the fixed scenario is M6 (warmest-month temperature; lowest AIC in 70% of trees) rather than M5 (average monthly temperature), whereas the non-breeding season selects M5 under both scenarios. Second, the temperature × migration interaction in the breeding season is $\beta = 0.019$ [0.006, 0.031] under the fixed scenario, an interval excluding zero, compared with $\beta = 0.011$ [−0.002, 0.024] under the variable scenario. Third, the breeding-temperature × seasonal-shift interaction likewise excludes zero under the fixed scenario only. We interpret these differences as sensitivity of the seasonal-window definition rather than as competing estimates.

A. AIC model comparison across 50 trees

Season	Model	Temp metric	Interactions	variable: mean AIC	variable: dAIC	variable: Akaike w	variable: best in % of trees	fixed: mean AIC	fixed: dAIC	fixed: Akaike w	fixed: best in % of trees
BR	M5	mean_tavg	yes	125.4	0.05	0.751	96	142.6	4.5	0.312	30
BR	M2	mean_tavg	no	128.1	2.71	0.233	4	147.7	9.59	0.023	0
BR	M6	max_tavg	yes	139.5	14.18	0.016	0	140.1	1.92	0.651	70
BR	M3	max_tavg	no	149.2	23.83	0	0	148.9	10.72	0.013	0
BR	M4	min_tavg	yes	167.1	41.76	0	0	189.8	51.67	0	0
BR	M1	min_tavg	no	174.4	49.06	0	0	195.5	57.33	0	0
NR	M5	mean_tavg	yes	121.4	0.01	0.91	98	122	0	0.921	100
NR	M2	mean_tavg	no	126.8	5.38	0.09	2	127.7	5.7	0.078	0
NR	M6	max_tavg	yes	143.3	21.92	0	0	143.5	21.49	0.001	0
NR	M3	max_tavg	no	153	31.62	0	0	156.9	34.85	0	0
NR	M4	min_tavg	yes	153.7	32.32	0	0	153.8	31.78	0	0
NR	M1	min_tavg	no	169.4	48.02	0	0	169.4	47.38	0	0

B. Standardised fixed-effect coefficients (beta [95% CI])

Season	Model	Term	variable scenario	fixed scenario
BR	M5	Intercept	2.339 [1.433, 3.245]	2.339 [1.433, 3.246]
BR	M5	Migration (migratory vs resident)	-0.030 [-0.049, -0.011]	-0.028 [-0.047, -0.009]
BR	M5	Precipitation	0.014 [0.008, 0.021]	0.015 [0.008, 0.022]
BR	M5	Precipitation × Migration	-0.012 [-0.031, 0.008]	-0.014 [-0.034, 0.005]
BR	M5	Temperature	-0.040 [-0.049, -0.030]	-0.041 [-0.051, -0.031]
BR	M5	Temperature × Migration	0.011 [-0.002, 0.024]	0.019 [0.006, 0.031]
BR	M5	Temperature × Precipitation	0.007 [-0.000, 0.014]	0.005 [-0.002, 0.012]
NR	M5	Intercept	2.338 [1.432, 3.244]	2.338 [1.432, 3.244]
NR	M5	Migration (migratory vs resident)	-0.026 [-0.045, -0.007]	-0.026 [-0.045, -0.007]
NR	M5	Precipitation	0.014 [0.007, 0.021]	0.014 [0.007, 0.021]
NR	M5	Precipitation × Migration	-0.014 [-0.031, 0.003]	-0.014 [-0.032, 0.003]
NR	M5	Temperature	-0.040 [-0.050, -0.031]	-0.042 [-0.052, -0.032]
NR	M5	Temperature × Migration	0.011 [-0.001, 0.023]	0.012 [-0.000, 0.024]
NR	M5	Temperature × Precipitation	0.007 [0.000, 0.014]	0.007 [0.000, 0.014]
BR	M2	Intercept	2.341 [1.435, 3.247]	2.341 [1.435, 3.247]
BR	M2	Migration (migratory vs resident)	-0.028 [-0.044, -0.012]	-0.028 [-0.044, -0.012]
BR	M2	Precipitation	0.015 [0.009, 0.022]	0.015 [0.009, 0.021]
BR	M2	Temperature	-0.041 [-0.048, -0.033]	-0.038 [-0.045, -0.030]
NR	M2	Intercept	2.339 [1.434, 3.245]	2.340 [1.434, 3.246]
NR	M2	Migration (migratory vs resident)	-0.019 [-0.034, -0.004]	-0.019 [-0.035, -0.004]
NR	M2	Precipitation	0.014 [0.008, 0.021]	0.014 [0.008, 0.021]
NR	M2	Temperature	-0.041 [-0.048, -0.034]	-0.042 [-0.049, -0.035]

C. Variance components and Pagel's lambda (estimate [95% CI])

Season	Model	Component	variable scenario	fixed scenario
BR	M5	Pagel's lambda	0.989 [0.980, 0.994]	0.989 [0.980, 0.994]
BR	M5	sigma^2	0.008 [0.007, 0.008]	0.008 [0.007, 0.008]
BR	M5	sigma_E	0.095 [0.086, 0.105]	0.095 [0.086, 0.105]
BR	M5	sigma_phylo	0.904 [0.680, 1.202]	0.905 [0.680, 1.203]
NR	M5	Pagel's lambda	0.989 [0.980, 0.994]	0.989 [0.980, 0.994]
NR	M5	sigma^2	0.008 [0.007, 0.008]	0.008 [0.007, 0.008]
NR	M5	sigma_E	0.095 [0.086, 0.104]	0.095 [0.086, 0.104]
NR	M5	sigma_phylo	0.904 [0.680, 1.203]	0.904 [0.680, 1.203]
BR	M2	Pagel's lambda	0.989 [0.980, 0.994]	0.989 [0.980, 0.994]
BR	M2	sigma^2	0.008 [0.007, 0.008]	0.008 [0.007, 0.008]
BR	M2	sigma_E	0.095 [0.086, 0.105]	0.095 [0.086, 0.105]
BR	M2	sigma_phylo	0.905 [0.680, 1.203]	0.905 [0.681, 1.203]
NR	M2	Pagel's lambda	0.989 [0.980, 0.994]	0.989 [0.980, 0.994]
NR	M2	sigma^2	0.008 [0.007, 0.008]	0.008 [0.007, 0.008]
NR	M2	sigma_E	0.095 [0.086, 0.105]	0.095 [0.086, 0.105]
NR	M2	sigma_phylo	0.904 [0.680, 1.202]	0.904 [0.680, 1.203]

D. Within-migrant seasonal-shift models (beta [95% CI], n = 1805)

Temp metric	Model	Term	variable scenario	fixed scenario
mean_tavg	base	Breeding temperature	-0.039 [-0.053, -0.025]	-0.028 [-0.041, -0.015]
mean_tavg	base	Breeding precipitation	-0.008 [-0.033, 0.016]	-0.009 [-0.033, 0.015]
mean_tavg	shift_main	Breeding temperature	-0.051 [-0.065, -0.036]	-0.047 [-0.061, -0.032]
mean_tavg	shift_main	Seasonal temperature shift (NR-BR)	-0.038 [-0.054, -0.023]	-0.050 [-0.067, -0.033]
mean_tavg	shift_main	Breeding precipitation	-0.012 [-0.037, 0.013]	-0.015 [-0.040, 0.011]
mean_tavg	shift_main	Seasonal precipitation shift (NR-BR)	0.003 [-0.011, 0.016]	0.003 [-0.010, 0.017]
mean_tavg	shift_interaction	Breeding temperature	-0.045 [-0.061, -0.029]	-0.039 [-0.054, -0.023]
mean_tavg	shift_interaction	Seasonal temperature shift (NR-BR)	-0.017 [-0.048, 0.014]	-0.014 [-0.045, 0.017]
mean_tavg	shift_interaction	Breeding precipitation	-0.013 [-0.038, 0.012]	-0.016 [-0.041, 0.009]
mean_tavg	shift_interaction	Seasonal precipitation shift (NR-BR)	0.003 [-0.011, 0.016]	0.004 [-0.009, 0.018]
mean_tavg	shift_interaction	Breeding temperature x seasonal shift	0.010 [-0.002, 0.023]	0.015 [0.004, 0.025]
min_tavg	base	Breeding temperature	-0.038 [-0.052, -0.024]	-0.022 [-0.035, -0.010]
min_tavg	base	Breeding precipitation	-0.006 [-0.030, 0.019]	-0.010 [-0.035, 0.015]
min_tavg	shift_main	Breeding temperature	-0.065 [-0.082, -0.049]	-0.064 [-0.081, -0.047]
min_tavg	shift_main	Seasonal temperature shift (NR-BR)	-0.057 [-0.075, -0.039]	-0.080 [-0.101, -0.059]
min_tavg	shift_main	Breeding precipitation	-0.015 [-0.040, 0.011]	-0.020 [-0.046, 0.005]
min_tavg	shift_main	Seasonal precipitation shift (NR-BR)	0.000 [-0.013, 0.013]	0.000 [-0.013, 0.014]
min_tavg	shift_interaction	Breeding temperature	-0.057 [-0.076, -0.037]	-0.053 [-0.071, -0.035]
min_tavg	shift_interaction	Seasonal temperature shift (NR-BR)	-0.029 [-0.068, 0.010]	-0.027 [-0.064, 0.010]

min_tavg	shift_interaction	Breeding precipitation	-0.014 [-0.040, 0.011]	-0.018 [-0.043, 0.008]
min_tavg	shift_interaction	Seasonal precipitation shift (NR-BR)	0.002 [-0.011, 0.015]	0.006 [-0.008, 0.019]
min_tavg	shift_interaction	Breeding temperature x seasonal shift	0.013 [-0.003, 0.028]	0.019 [0.008, 0.030]

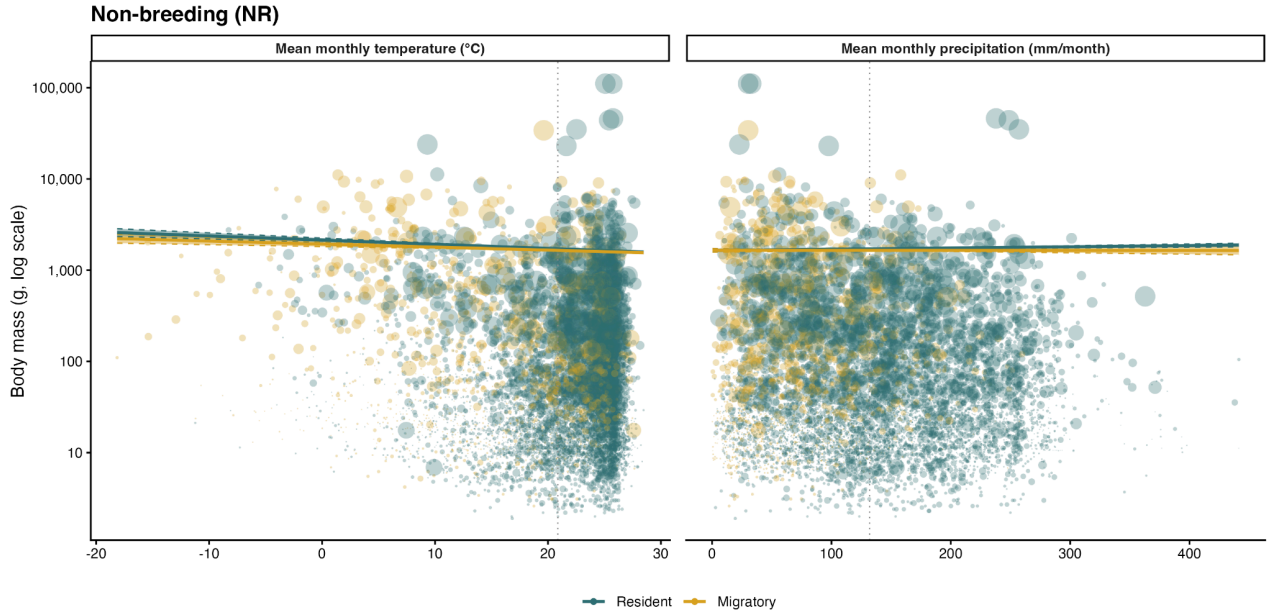

Figure S1. Relationships between body mass and non-breeding-season climatic exposure. Panels show non-breeding-season temperature (A) and non-breeding-season precipitation (B). Points, lines, shaded wedges, and colours are as in Figure 3. Resident species are assigned year-round climatic exposure, so their values are identical to those in the breeding-season figure (Figure 3); migratory species are shown at their non-breeding-season climatic exposure.